Shielding Effect for Workability Improvement in Offshore Lifting Operations

Auteur : Anwar, Osama Bin
Promoteur(s) : Rigo, Philippe
Faculté : Faculté des Sciences appliquées
Diplôme : Master : ingénieur civil mécanicien, à finalité spécialisée en "Advanced Ship Design"
Année académique : 2023-2024
URI/URL : http://hdl.handle.net/2268.2/22253

Shielding Effect for Workability Improvement in Offshore Lifting Operations

Master Thesis

Submitted on August 05, 2023

by Osama Bin Anwar

osama.anwar@uni-rostock.de

Student ID No.: 223202142

Reviewer

Prof. Dr.-Ing. Florian Sprenger

florian.sprenger@uni-rostock.de

University of Rostock

Albert-Einstein-Str 2, 18059 Rostock, Germany

Reviewer

Pedro Mendonca

pedro.mendonca@jandenul.com

Jan De Nul Group

Tragel 60, 9308 Hofstade-Aalst, Belgium

EMShip+ Program

Advanced Design of Ships and Offshore Structures

Academic year 2023-2024

Shielding Effect for Workability Improvement in offshore lifting operations

The work in this thesis was carried out in:

Jan De Nul NV
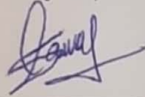Tragel 60
9308 Hofstade-Aalst
Belgium

Faculty Supervisor:	Dr.-Ing. Florian Sprenger (University of Rostock, Germany)
Direct Supervisor:	Pedro Mendonca, Marine Design Engineer (Jan De Nul Group, Belgium)

This document was set with LaTeX on July 25, 2024

Declaration of Authorship

Acknowledgement

First of all, I extend my gratitude to the Almighty God for his never ending blessings and strength, which proved pivotal in guiding me not only through this thesis but all the challenges I encounter in my life.

To my father, who has been a source of constant support throughout my life. His wisdom and encouragement have been the foundation of my determination and strength.

To my dearest Mother, who was very supportive of me in every thick and thin and celebrated all my accomplishments with me. Her memory makes me keep going. Though she is not with us, her spirit and love still serves as guiding light for me.

To Professor Philippe Rigo, who believed in my abilities and potential and let me have this opportunity to receive Erasmus Mundus Scholarship. His recommendation also made the way for my internship and master thesis at Jan de Nul, for which I am very thankful.

Lastly, I would like to thank my supervisors Thomas Muysewinkel, Pedro Mendonça, and Professor Florian Sprenger for their expert guidance and constant support throughout the development of this thesis. Their expertise and feedback were invaluable, helping me overcome challenges and refine my work to its current standard.

This thesis is not just my own but a reflection of the unwavering love and support of these remarkable individuals. I am profoundly thankful to each of you.

Abstract

This thesis explains the effect of wave shielding ability of a large vessel on the workability of offshore lifting operations. Monopile and jacket structures are considered for this study. The goal is to enhance the operational window and safety of these operations by analyzing in-depth how much effective is vessel shielding.

A detailed methodology is deveoped and employed including hydrostatic stability evaluation of vessel, sea keeping analysis in Ansys Aqwa, and time domain dynamic simulations in Orcaflex. Vessel, monopile, jacket, crane, and relevant sea states are modeled using Ansys Aqwa and Orcaflex to simulate reaslistic conditions in order to check their influence on actual lifting operations.

The results show that vessel sheilding significantly improves the offshore workability for specific wave directions and especially for lower wave periods. The effect of shielding on the type of structure to be installed also varies based on structure type. Workability enhances much more for monopile installation as compared to jacket installation if shielding is considered.

These findings highlight how important it is to take into account the designs of offshore structures when looking at the benefits of wave shielding. The study proves useful for making offshore lifting activities better, which could lower risks, cut downtime, and save costs. By allowing operations to continue in a wider range of weather conditions, shielding effect appears to be a good way to make offshore installation projects safer and cost friendly.

Keywords: Offshore lifting, vessel shielding, workability, hydrostatic stability, dynamic simulations

Table of Content

List of Figures

List of Tables

List of Abbreviations

Abbreviation	Meaning
COG	Center of Gravity
DAF	Dynamic Amplification Factor
DLL	Dynamic Link Library
DNV	Det Norske Veritas
DP	Dynamic Positioning
EWEA	European Wind Energy Association
EU	European Union
FPSO	Floating Production Storage and Offloading
GBS	Gravity Based Structures
IEA	International Energy Agency
IMO	International Maritime Organization
JDN	Jan de Nul
LCG	Longitudinal Center of Gravity
MP	Monopile
PS	Portside
RAO	Response Amplitude Operator
RNA	Rotor Nacelle Assembly
RP	Recommended Practice
SB	Starboard Side
SCR	Steel Catenary Risers
SIMO	Single Input Multiple Output
SPM	Single Point Mooring
TCG	Transverse Center of Gravity
TLP	Tension Leg Platforms
TTR	Top Tensioned Riser
VCG	Vertical Center of Gravity

List of Formulas

Symbol	Unit	Meaning
GM	m	Metacentric Height
H_s	m	Significant Wave Height
I_{xx}	m^4	Moment of Inertia around x axis
I_{yy}	m^4	Moment of Inertia around y axis
I_{zz}	m^4	Moment of Inertia around z axis
K_{xx}	m	Radius of gyration around x axis
K_{yy}	m	Radius of gyration around y axis
K_{zz}	m	Radius of gyration around z axis
γ	$--$	Peak Enhancement Factor
T	s	Pendulum Natural Time Period
T_p	s	Wave Peak Period
T_z	s	Zero Upcrossing Period

1

Introduction

1.1 Background

The pressing need for sustainable and dependable energy sources is intensified by global warming and the ongoing energy crisis. It is projected that by 2040, 20% of global electricity will come from renewable sources EWEA [5]. Wind power is particularly reliable due to certain advantages it has e.g. availability(means wind energy has low delays because is almost always present), cost-effectiveness, and manageable risk.

For few decades, onshore wind turbines have been utilized to generate green energy [6, 7]. In contrast, offshore wind energy provides several key benefits, like stronger wind velocities, less turbulence, reduced noise pollution for people because of remote locations, and the ability to transport and install larger turbines [8]. This has led to a significant increase in offshore wind development over the last twenty years, with further expansion expected as shown in figure 1.1. In Europe, the total installed capacity of offshore wind turbines is 25 GW. The total number of installed wind turbines exceeds 5000 across 12 countries offshore wind [9].
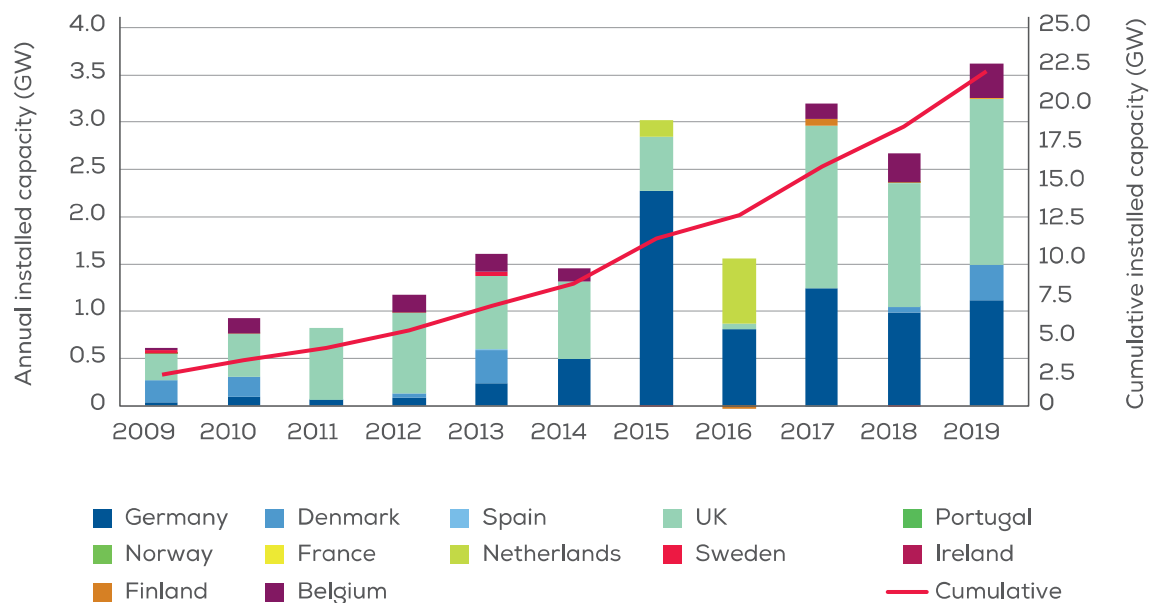
Figure 1.1: Annual offshore wind installation by country WindEurope [1]

However, the offshore wind sector faces considerable challenges. Research shows that the initial investment for offshore wind farms is more than double that of onshore projects [2]. Offshore turbines, while based on land designs, must be specially adapted to withstand aquatic corrosion and harsh marine conditions [10]. The increased expenses for offshore projects stem from the high costs of building sea-based foundations, as well as the complexities of transporting and installing these foundations, equipment, and turbines. Additionally, costs

associated with operation and maintenance are significantly higher [11].

Figure 1.2 illustrates the cost distribution for both land-based and offshore wind turbines. The costs associated with installing and assembling offshore wind turbines can represent up to 20% of the total capital expenditure, in contrast to only 6% for their land-based counterparts[2]. Offshore operations are considerably more complex and costly than onshore activities, posing greater financial and engineering challenges. The primary issue lies in the uncertainties associated with the harsh offshore environmental conditions, which impose greater structural loads and increase risks. Given the narrow profit margins in the offshore wind sector, it is crucial to reduce installation expenses by refining methodologies during the design and planning stages.
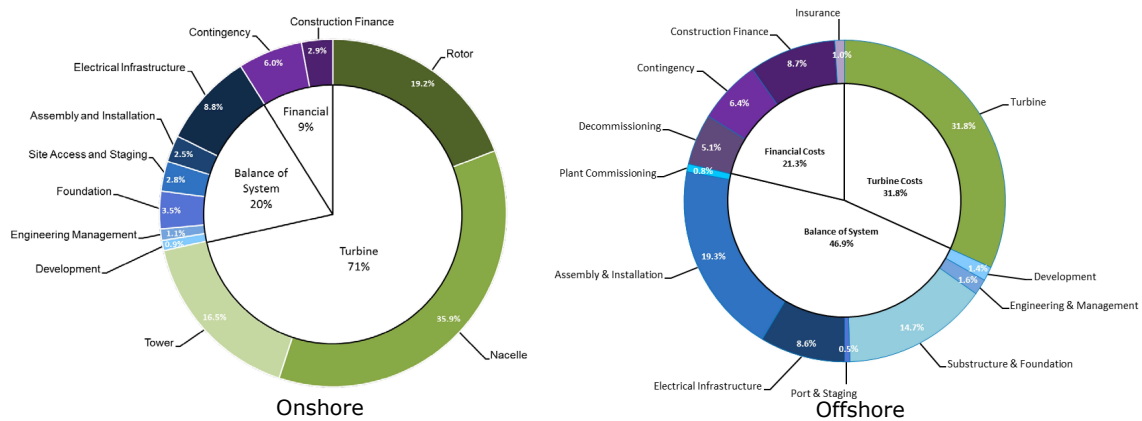
Figure 1.2: Cost breakdown comparison between offshore and onshore wind turbines [2]

Offshore wind farms are progressively being established farther from the coast and in deeper waters, as depicted in Figure 1.3 , where the size of bubble is proportional to wind farm's capacity. By the end of 2014, the average water depth for operational wind farms was 22.4 meters, and wind farms were around 32 kms from shore on an average [5].
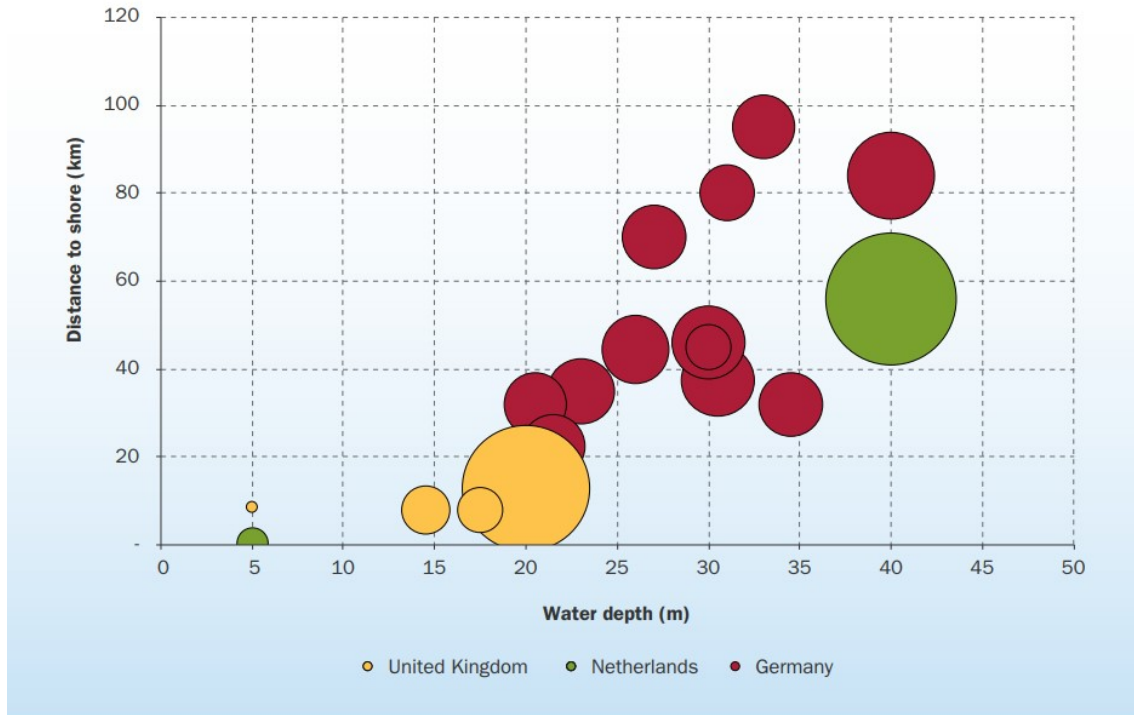
Figure 1.3: Average water depth and distance to shore of various offshore wind farms (Bubble size representing windfarm capacity.) [5]

Current projects that are under construction, approved, or planned suggest that these average depths and distances will continue to increase, thereby presenting greater challenges for transportation, installation, operation, and maintenance of these wind farms. Consequently, the capital costs for offshore wind farms in Europe have risen in recent years, as shown in Figure 1.4 and it totally make sense. To cut these costs, a better comprehension of the principal risks associated with offshore wind projects is required.
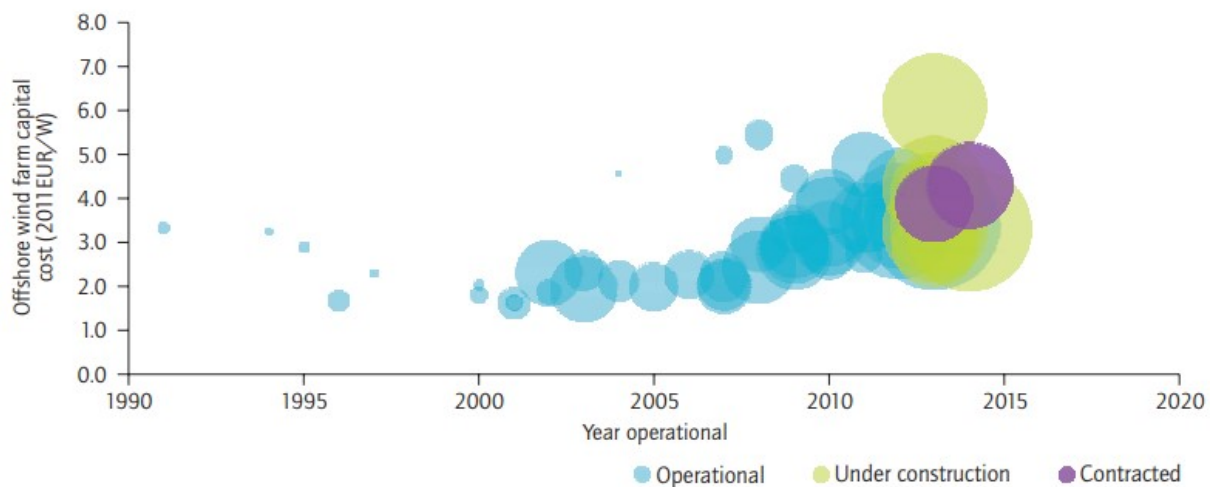
Figure 1.4: Capital cost trend of european wind farms year by year [3]

An offshore wind turbine is composed of the Rotor Nacelle Assembly(RNA), the tower,

and a bottom structure to support it. Figure 1.5 displays different foundation types for these turbines. Monopiles are the most prevalent foundation types for depths up to 40 meters due to their straight forward design and lower costs associated with manufacturing and installation Thomsen [12]. Gravity-based structures (GBS) are very good when it comes to shallow waters where pile driving is cumbersome, with the deepest GBS installation reaching 28 meters at Thornton Bank wind farm [13]. Jackets and tripods are capable of meeting the necessary strength for depths up to 60 meters [14]. For depths exceeding 100 meters, floating platforms are likely to be more economical, with three main types currently being explored as depicted in Figure 1.5 .
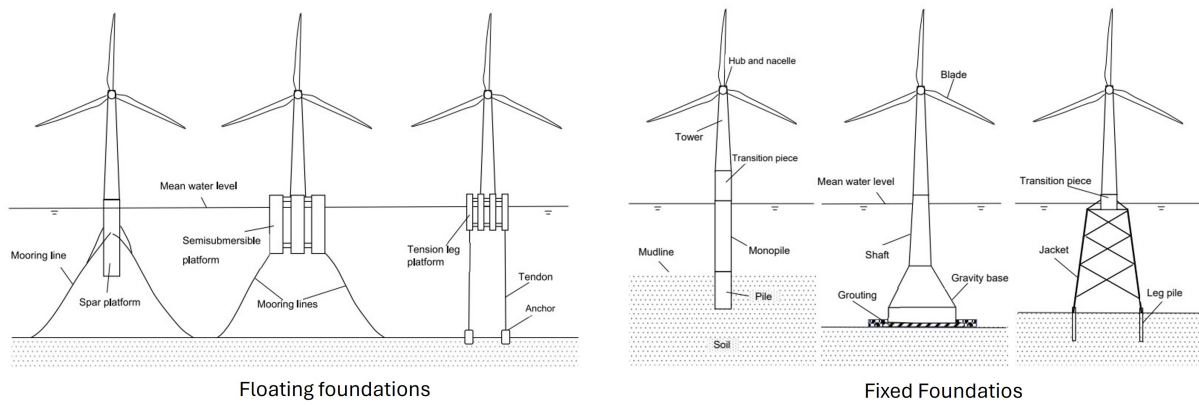
Figure 1.5: Different type of foundations for offshore wind turbines [4]

2

Motivation

2.1 Problem statement

During foundation placement, hydrodynamic forces exert significant loads on structures as they are lowered through the splash zone. Splash zone is the horozontal patch of water which encompasses the location where offshore structure e.g. monopile is lowered. When using a floating installation vessel, the lifting mechanism becomes particularly susceptible to wave loads, necessitating a thorough response analysis during the planning stage. For the installation of turbine components, considerations include height of the lifting and the potential for pendulum movements caused by wind. It is essential to ensure that lifting at different elevations remain within the crane's lifting capacity and that pendulum movements stay within safe operational limits.

Operational weather criteria significantly affect system downtime. The most considerable downtime during offshore lifting operations results from wave conditions during foundation lifting or wind conditions during RNA installation. Positioning jack-ups also contributes to significant downtime. This is because they are more sensitive to change in weather conditions especially during jacking up operations. Furthermore, soil conditions also play their role in down time. Consequently, more floating installations are being utilized for foundation placement to expand the operational weather window, allowing for quicker transit and repositioning. Nevertheless, for the installation of turbines, jack-ups are still the preferred vessels. Expanding the weather window is crucial for reducing costs in the installation of wind farms that consist of multiple structures.

Based on the fact that more and more offshore wind farms are to be installed in the future, these problems associated with offshore wind turbine installation needs to be addressed and measures are to be taken in order to make the offshore lifting or lowering through splash zone becomes more efficient, reliable, safe and feasible. For this, some solution regarding the widening of weather window for these installations is needed.

2.2 Research Objective

Based on the complexities and challenges inherent in the installation of offshore wind turbines, this thesis explores an innovative approach to enhance operational workability through the use of vessel shielding. Normally weather window width is enhanced using dynamic positioning of the vessel and by the use of motion compensation devices. By positioning installation vessel in such a way that they block incoming wave action, the objective is to create a significantly calmer sea state around the installation site. This method holds potential for enhancing the

process by reducing the impact of harsh marine conditions on lifting operations, which is crucial for ensuring the efficiency and safety of construction activities.

The research objective that is dealt with in this thesis is to have a thorough analysis of vessel shielding effect and to check how effective it is in enhancing the workability of offshore lifting/installation operations. This thesis checks the shielding effect by variations in vessel positioning and its effect on the allowable wave height. The effect of vessel shielding is studied in the context of monopile and jacket lowering operation. Lowering operation is studied by comparing both the shielded and unshielded case and then effect of shielding on workability is observed.

The question about enhacement of workability is studied by using the dynamic simulations. Wave dynamics like diffraction due to vessel presence and radiation due to vessel motion is studied and its effect on the sea state is observed by using these dynamic simulations. This checks how the interaction between vessel and incoming waves effect the operational window.

By having this study done, a measure of upto what extent the allowable wave height can be tolerated is evaluated. So operational safety as well as weather window can get widended if this study yields good results.

3

State of the art

The steps involving the building of an offshore wind farm includes carriage and installation of wind turbine foundations, wind turbines themselves, offshore substations and cables. The predominant technique for installing foundations is the use of heavy lifting operations, typically performed with floating vessels or jack-up vessels. For bigger substations, the floating installation presents an alternative option [15]. Typically, turbine components are hoisted and positioned using jack-up vessels. Installation processes involve multiple types of activities and are often time consuming. Minimizing time and costs for each activity can significantly reduce the overall expense of the operation and, consequently, the entire wind farm. Thus, selecting appropriate methods and equipment is critical for efficient installation planning.

Monopiles are typically transported either using a barge or with the help of installation of vessel, or they are capped and transported via wet towing [16]. As the dimensions and mass of these monopiles increase, employing large installation vessels for their transport becomes costly. Alternatively, the wet tow method has been utilized effectively. This approach to floating a single monopile has been successfully implemented during the installation processes of two wind farms [17]. Moreover, transporting multiple monopiles in a single journey is feasible with the appropriate connection between them.

The process of installing monopiles typically involves two principal phases: upending and then drilling of the piles. Performing a combined wet-tow and upending operation in water can be managed by cranes of lower capacity than those needed for transport and upending on the vessel itself. However, upending monopiles in water is more susceptible to weather conditions compared to on-board operations. The key procedures in monopile installation are the upending, lowering into position, and the driving process. It is crucial to maintain the monopile's vertical alignment during the driving process to ensure accuracy.

Sarkar [18] has proposed a method to decouple the installation activities from the movements of the floating vessel by employing a pre-installed submerged structure for support. The monopiles, which are end-capped and transported through wet towing, are then supported against the dynamic forces of waves and currents by this support structure during their initial drilling into the seabed.

Lifting operations serve as a primary method for deploying monopiles and various other offshore infrastructures. To predict the behavior of these operations, numerical simulations are frequently utilized, addressing the dynamic responses of a range of installations including sub-sea templates [19], suction anchors [20], foundation structures, platform topsides, and components of wind turbines [21]. Additionally, several experimental investigations have been carried out to accurately determine hydrodynamic coefficients, such as the added mass

and damping coefficient of piles [22], or to adjust critical factors within numerical models, such as the damping or stiffness of essential supporting structures within the lifting equipment [23].

In operations where monopiles are lowered from aerial positions through the splash zone and down to the seabed, the dynamic characteristics of the system continuously vary. Such processes, defined by their transient or significantly non-linear behaviors, require numerical and analytical methods distinct from those applied in stationary conditions [24].

In operations where heavy loads such as monopiles are lowered by floating vessels, understanding the hydrodynamic interactions that occur due to wave activity is critical. Research into heavy lifting operations within the oil and gas sector has explored the shielding effect of using large semi-submersible crane vessels to shield smaller transport barges [25, 26, 27]. These studies indicate that while the crane tip's reactions are not influenced significantly by hydrodynamic forces, the smaller barge's responses are much impacted due to its relatively smaller size compared to the crane vessel. Thus, the proximity of two floating structures influences their dynamic responses and must be considered in response assessments.

In situations where a monopile is lowered using a floating vessel, the hydrodynamic effects exerted by the relatively small monopile on the larger vessel are generally negligible. Nonetheless, the vessel's capacity to alter wave patterns around the monopile is pronounced and should not be overlooked. This difference results from the wave fields near the floating vessel being changed by diffraction and radiation effects, even when the incident waves are long-crested. Proper positioning of the lifting system and vessel relative to incoming waves can reduce the lifting system's exposure to wave impacts, leveraging what is known as wave shadow effects [28]. Therefore, examining the shielding effects provided by the vessel during lowering operations in wave-affected areas is essential for optimizing operational responses.

When smaller structures are located near a much larger floating body, it is crucial to consider the radiation and diffraction impacts on the fluid movements when determining the forces acting on the structure [29]. Typically, the process involves calculation of sea state disturbance RAOs to actually model the effect of presence of vessel as an obstacle to incoming waves and then to calculate the loads on the structure bing lowered based on this disturbed sea state. This method is applicable primarily when the lifting system maintains a constant mean position.

Nonetheless, the complexities of the system due to transient behaviors and inherent non-linearities suggest that the position of the objects being lowered will vary over time. Consequently, it becomes necessary to employ time-domain techniques to accurately model the entire lowering process, taking into account the shielding effects offered by the nearby vessel.

In these studies, the approach to account for shielding effects involved calculating the coupled hydrodynamic coefficients in the frequency domain while all elements maintained their average positions. This presupposes minimal movement within the system. Nonetheless, during ongoing lowering operations where the positions of the objects being lifted vary w.r.t time, this technique proves inadequate. One major challenge in this context is the significant motion that the load may undergo due to wave activity while being lowered Bai et al. [30]. developed a three-dimensional non-linear potential flow model to assess wave interactions

with fully submerged structures, whether static or under constrained movement, using a time-domain approach. They examined a scenario where a cylindrical load hung from a solid cable and was exposed to wave forces. Yet, this method has been restricted to regular wave patterns so far, and its simulation efficiency remains low. Its adaptability to more complex tasks or under irregular wave conditions for extended periods remains uncertain and is questionable.

Regarding the lifting of a monopile with a floating vessel, due to the size differential between the monopile compared to the vessel means the hydrodynamic impact of the monopile on the vessel is minimal and generally disregarded[31]. presented a strategy to consider the shielding provided by the installation vessel to a monopile throughout its lowering through splash zone. They applied Morison's equation to compute the wave forces on the monopile by interpolating sea state disturbances at specific wave points which lied in the splash zone. Findings indicated that the responses of the monopile are considerably diminished in shorter waves when shielding effects are considered. The research also suggested that optimizing the vessel's orientation can further minimize responses, leveraging these shielding effects, although the analysis was limited to long-crested waves.

Previous research has focused on refining numerical methods to more accurately simulate the lifting operations of monopiles, particularly emphasizing the non-stationary aspects of these processes. Certain assumptions were made within the numerical models in those researches. For example, studies have shown that any interaction between vessel and monopile can be ignored while checking the effects of monopile radiation damping and in this way, hydrodynamic forces on the vessel are simplified in reaction to the excitation due to incoming waves[32]. Furthermore, these studies did not consider the effect of short crestedness of waves as noted by DNV[33]. On top of that, these said studies did not investigate the allowable sea state which are necessary for planning the operation efficiently to reduce the operational costs.

Generally when lifting analysis is performed, it is a practice to ignore the hydrodynamic interation between the structures that are submerged and to simplify the model as much as possible by having steady state approximations to model the transient behaviours. But these simplifications can yield erroneous results. Actual effects produced by these simplifications and consequently efficiency of operations are yet to be studied in order to check if they yield over conservative results that will increase the expenses or they give overly tolerant results that can involve risks with the operations.

The installation process is studied for both the monopile and jacket case and comparisons are made [34]. In these installation analysis, effects due to vessel shielding for both structures acroos different wind farms are also studied. How the wave-structure interaction is influenced by incoming wave directions and wave peak periods, and in turn the variation in RAOs are investigated in these studies. The extract from these studies in that in case of monopile installation, the sea state experienced by it is very less as compared to jacket installation in case of shorter wave peak periods and waves coming from quartering direction.

In previous researches, external dynamic link library (DLL) is integrated in (SIMO) system to calculate hydrodynamic forces on monopile and jacket. In this method, the effect of vessel

shielding on the area surrounding the monopile or jacket is kept under consideration in order to have the precise information about how vessel presence is affecting the sea state and in turn the forces on structures to be installed.

The findings from the study provided compelling evidence that the shielding provided by the vessel mitigated the responses of monopiles in short-wave environments, particularly when near quartering seas. This mitigation effect is observed to diminish in longer wave scenarios, where the induced motions from the vessel can intensify the overall dynamics of the system, potentially complicating the lifting operations. In contrast, the responses of the jacket structures are predominantly governed by the vessel's movements, even in shorter waves. This suggests a minimal impact from the shielding, indicating that the physical characteristics and positioning of the jackets diminish the effectiveness of such shielding strategies.

The results of this study made sure that vessel shielding has promising effect on monopile response especially when it comes to short waves approaching the installation zone from quartering direction. On the contrary, we can't see so much effect of vessel presence in case of long waves because for higher periods, vessel motion is also very high and it renders the lifting operation difficult to execute. So, the monopile motion is governed by vessel movement only in case of short waves but for jacket, its motion is influenced by vessel in both long and short waves. This means when it comes to jackets, the effect of vessel shielding is not so much.

Torgeir [35] in her research suggested that while planning monopile installation, effect of vessel shielding should be taken under consideration. She recommended optimizing the heading angles to leverage the protective effects of shielding, which could significantly broaden the operational windows under varying sea conditions. This strategic approach is poised to enhance safety, reduce operational risks, and improve efficiency in monopile installations. Conversely, the findings suggest that shielding effects have a negligible impact on jacket installations. Therefore, for jackets, it is often practical to overlook shielding considerations in planning, especially under conditions where the vessel's own movements dominate the operational dynamics.

In essence, this comprehensive analysis underscored the necessity to tailor shielding strategies according to the specific structural characteristics and operational contexts of the offshore installations. By doing so, it is possible to maximize the effectiveness of installation operations while ensuring optimal use of resources and minimizing environmental impacts.

4

Methodology

This chapter outlines the basis of design, definitions and systematic workflow adopted for the research conducted in this thesis. To provide a clear understanding of the processes involved, a flowchart is presented initially. This visual representation serves as an informative overview, for a detailed exploration of each step within the workflow. Subsequently, each phase of the workflow is explained in detail, offering deeper insights into the methodologies employed and their significance in advancing the study. This structured approach not only enhances the clarity of the research approach but also facilitates a thorough understanding of the procedures and analytical techniques integral to this study.

4.1 Basis of Design

4.1.1 Unit System

All units are metric unless specified otherwise.

- Mass: 1t = 1000 kg
- Sea Water Density: 1.025 t/m^3
- Air Density: 1.343 kg/m^3
- Acceleration due to gravity: 9.8 m/s^2

4.1.2 Coordinate System

The Coordinate system used throughout is right handed unless otherwise specified. Coordinate system can be seen in figure 4.1 below.
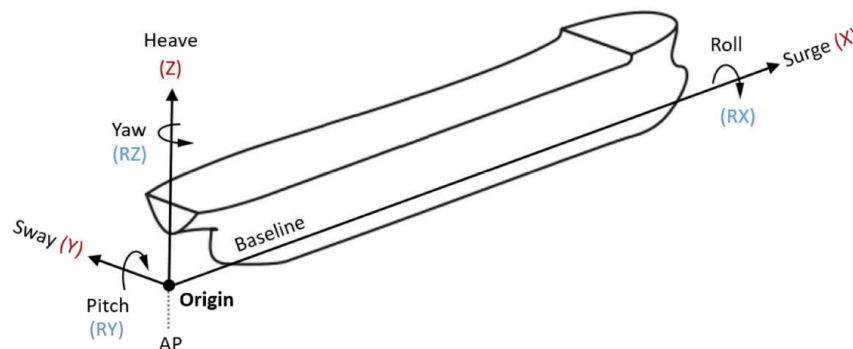
Figure 4.1: Coordinate System

The convention in **ANSYS AQWA** and **Orcaflex** for the origin of coordinate system X, Y, and Z is as follows:

- X = 0 at zero frame, positive x-coordinats in forward directions
- Y = 0 at centre line of vessel(CL), positive y-coordinates towards **portside(PS)**.
- Z = 0 at **waterline** of the vessel(WL), positive z-coordinates in upward direction

The convention in **SARC PIAS** for the origin of coordinate system X, Y, and Z is as follows:

- X = 0 at zero frame, positive x-coordinats in forward directions
- Y = 0 at centre line of vessel(CL), positive y-coordinates towards **starboard side(SB)**.
- Z = 0 at **baseline** of the vessel(BL), positive z-coordinates in upward direction

The wave direction in AQWA and Orcaflex is defined as the angle from the positive global X axis to the direction in which the wave is travelling, measured anti-clockwise when seen from the top. An example of wave/current/wind heading is shown in figure 4.2

- 0 degrees = Stern waves (following waves)
- 90 degrees = SB beam waves
- 180 degrees = Head Waves (Head Seas)
- 270 degrees = PS beam waves
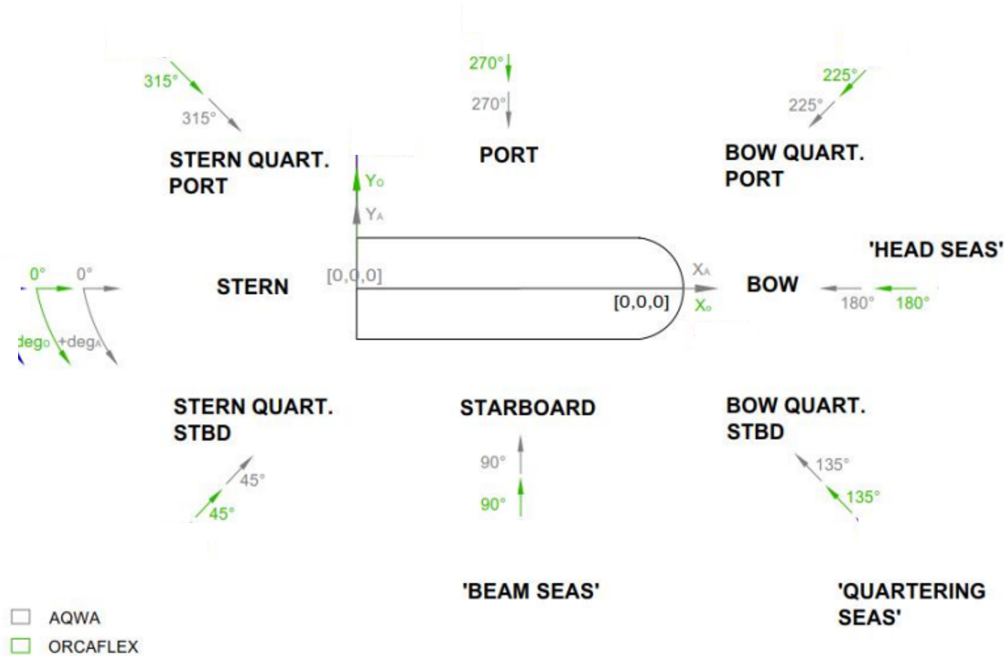
Figure 4.2: Wave conventions

4.2 Definitions

This section contains all the information regarding definitions of the parameters used in this thesis.

4.2.1 Significant Wave Height

The significant wave height is the average of the highest one third of the wave peaks in an irregular sea. In the following, wave height refers to the significant wave height H_s (crest to trough) unless mentioned otherwise.

4.2.2 Wave Period

The peak period, T_p, is defined as the irregular wave period where the wave spectrum energy is maximum. Unless mentioned otherwise, the wave period refers to the irregular peak wave period. The zero up-crossing period, T_z, is the mean irregular wave period between two consecutive upward wave crossings with the static water level.

4.2.3 Natural Period

The natural periods can be calculated with the following formula:

$$T_n = 2 * \pi * \sqrt{\frac{m + a}{c}} \quad (s) \tag{4.1}$$

Where

T_n: The undamped natural period of a certain mode of motion.
m: The coresponding element from the mass matrix.
a: The corresponding element from the added mass matrix.
c: The corresponding element from the stiffness matrix.

4.3 Vessel Specifications

This study is performed for the monopile installation at Borkum Riffgrund offshore wind-farm. The lifting vessel for this project is Jan de Nul's Les Alizés. "Les Alizés", is a DP2 Heavy Lift Crane Vessel, which is classified as an Offshore Construction Vessel designed for lifting operations [36]. It is equipped for unrestricted navigation and carries certifications like DYNAPOS-AM/AT-R (DP Class 2), Clean Ship ND07, and a Green passport EU, indicating high environmental standards.

The vessel sails under the Luxembourg flag and has following dimensions, including a length overall of 236.8 meters, a breadth of 52 meters, and a maximum draft of 10.5 meters. Its deadweight tonnage (DWT) is 61,000 tons.

Key to its operations is the crane system, manufactured by Huisman, which boasts a maximum lifting capacity of 5,000 tons at 36 meters with the main block, and an auxiliary block that can lift 1,500 tons at 46 meters radius. The auxiliary block is also capable of operating at significant depths, supporting operations up to 440 meters underwater.

The vessel's propulsion system includes Main Gen. Sets featuring Diesel Engines by MAN, capable of generating 6 x 7,200 kW, and supports environmental compliance with IMO Tier

III and Euro stage V standards. It has a maximum speed of 13 knots, supported by azimuth and bow thrusters for enhanced maneuverability.

Accommodation on the vessel is provided for crew, with 120 single and 15 double cabins. It also includes a heli deck capable of supporting helicopters like the Sikorsky S-61N, S-92, and Agusta-Westland EH-101.

Figure 4.3: Les Alizes loaded with monopiles

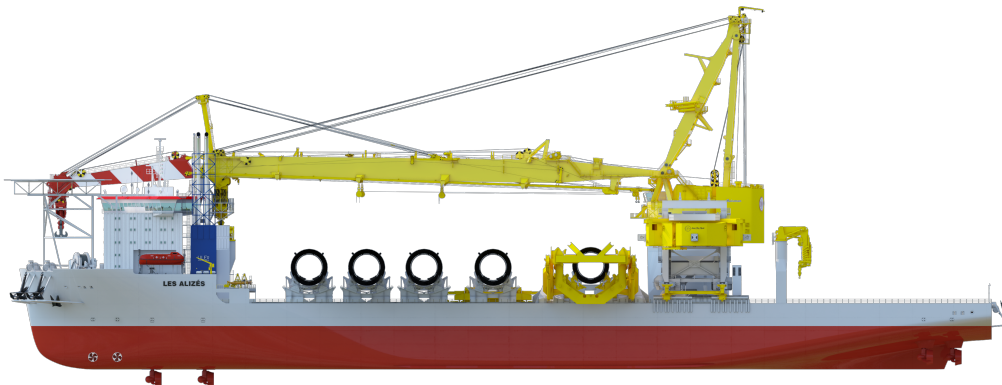**Figure 4.4:** Les Alizes Sideview

4.4 Lifting Plan

Lifting plan for this study is taken from offshore renewables department of JDN, it contains the configuration in which monopile is to be lowered in the splash zone. From lifting plan, the important information to extract is crane slew angle, crane radius, and crane boom angle. Figure **??** shows the visual representation of lifting plan.

4.5 Deck Layout

The deck layout of a vessel serves as an input data for stability software, defining the current loading conditions. This layout includes every component on board, along with its weight, contingency percentage, and the coordinates of its LCG, TCG, and VCG. It is important to ensure that the sign conventions for these coordinates in the deck layout align perfectly with those used by the stability software. If the conventions do not match, the data must be converted to a compatible form before being input into the software to ensure correctness of results.

The current thesis studies the deck layout of Les Alizes. This layout is provided by offshore renewables department at JDN. There is a difference in the convention of this layout and stability software SARC Pias. The transverse coordinate of COG are positive towards the PS in this layout but SARC considers positive coordinates towards SB side. So signs of these coordinates are reversed before feeding them into SARC.

4.6 Work Flowchart

Figure 4.5 shows the flow chart representing the whole workflow in an organized manner step by step. It depicts that the very first step is to determine the limiting criterias against which the effectiveness of shielding is to be studied. Once, this is established, vessel hydrostatic stability parameters are evaluated using stability software SARC PIAS.

After hydrostatic stability step, vessel sea keeping analysis is necessary for further proceedings. RAOs are calculated using diffraction solvers from ANSYS AQWA/(Orcawave). After RAOs evaluation, disturbance in the sea state (sea state RAOs) are determined in order to have a realistic modelling of the variation in sea state due to vessel presence.

The next step is the dynamic time domain simulations in Orcaflex to actually calcuate the results of monopile movement and all other limiting criterias to be evaluated.

After all the simulations performed, post processing of results is done in order to have meaningful conclusions regarding the objective. Post processing is done using Orcaflex spreadsheet to retrieve results simultaneously.

Finally, based on the retrieved results, the data will be used to make workability plots to convey proper information about the allowable wave heights for specific combination of wave peak periods and wave directions.
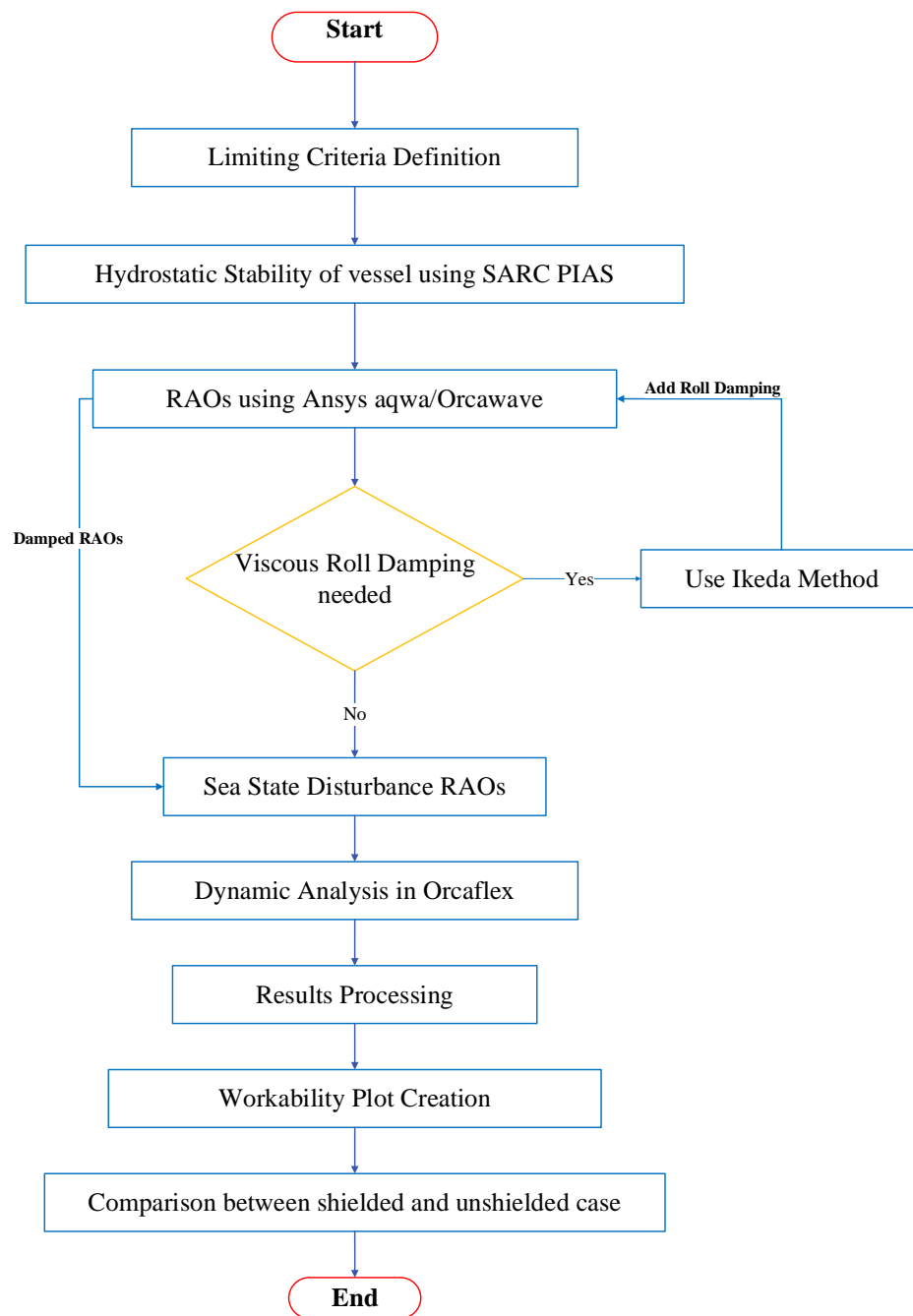
Figure 4.5: Workflow explanation flowchart

4.7 Limiting Criteria Definition

Limiting criteria are a necessary standard to check the effectiveness of shielding as to whether it is working or not. These limiting criteria are derived based on the operational limits of the equipments involved in the installation process. For example the horizontal motion of monopile is being limited by the gripper motion. Monopile gripper is the device which holds

the monopile in its place while lowering into the sea bed to maintain accurate positioning and to avoid vibrations. It stabilizes the monopile against lateral movements. In order to avoid monopile damage because of slam between monopile and gripper, limiting criteria is defined to monopile that will make sure that it shouldn't move more than specified gripper motion. Gripper can move 3 m in either horizontal direction, based on this, monopile horizontal motion is limited to 2.5 m in both horizontal directions. Generally whole operation is limited by a number of different criteria. Figure 4.6 shows the lowering of monopile while inside the gripper.
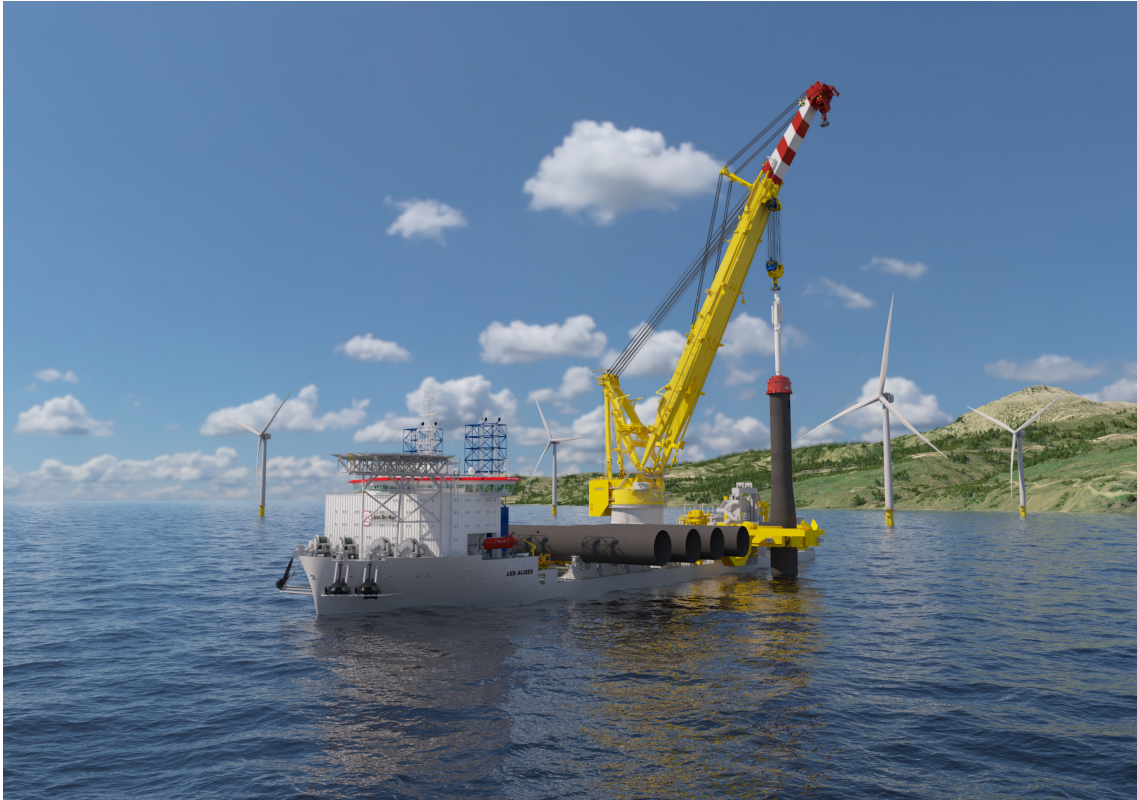
Figure 4.6: Monopile placed inside gripper and being lowered using Lez Alizes

Apart from monopile motion, crane leads(offlead and side lead) are also the limiting criteria because of their direct effect on monopile movement. DAF of crane is the last limiting criteria. This has been enforced because of crane load carrying capacity.

The results are analyzed against these comprehensive limiting criteria, which include the monopile horizontal motion (gripper's movement capacity), crane offlead, side lead, and DAF.

The results of dynamic simulations are evaluated against the said limiting criteria. These limiting criteria are tabulated in 4.1, providing a structured method for comparing the operational effectiveness under various conditions. This approach offers a clear, quantifiable measure of how effectively shielding enhances overall operational workability, ensuring a assessment of the operational dynamics.

Table 4.1: Limiting Criteria for this study

Limiting Criteria	Limiting Value
Monopile Horizontal Motion(m)	2.5
Crane Offlead(°)	2
Crane Sidelead(°)	3
Crane DAF(-)	1.15

4.8 Hydrostatic Stability Evaluation

For the assessment of hydrostatic stability within this study, the SARC PIAS software was utilized. Initially, to conduct a thorough stability analysis, it was good to establish an accurate loading condition and lifting plan. The loading condition is based on deck layout. These elements were sourced from the offshore renewable department. The loading condition specifies the components present on board, detailing their weights (inclusive of a 5% contingency) and the locations of their longitudinal, transverse, and vertical COG(LCG, TCG, and VCG).

The formulas to calculate local moment of inertia of each component having length (l), breadth(b), and height(h) can be calculated using formulas given in equations 4.2 to 4.4

$$I_{xx,local} = \frac{1}{12} \ * \ (b^2 + h^2) \ * \ m \tag{4.2}$$

$$I_{yy,local} = \frac{1}{12} \ * \ (l^2 + h^2) \ * \ m \tag{4.3}$$

$$I_{zz,local} = \frac{1}{12} \ * \ (b^2 + b^2) \ * \ m \tag{4.4}$$

To ensure the vessel's stability, ballast water tanks are there. These tanks require precise management to maintain stability throughout the operations. Figure 4.7 shows the general interface of SARC PIAS. The data input into SARC PIAS included a complete list of all components, their weights, and the coordinates for their COG based on the loading conditions. The lifting plan also dictated the crane's slew angle and radius, which were inputs for the stability software.
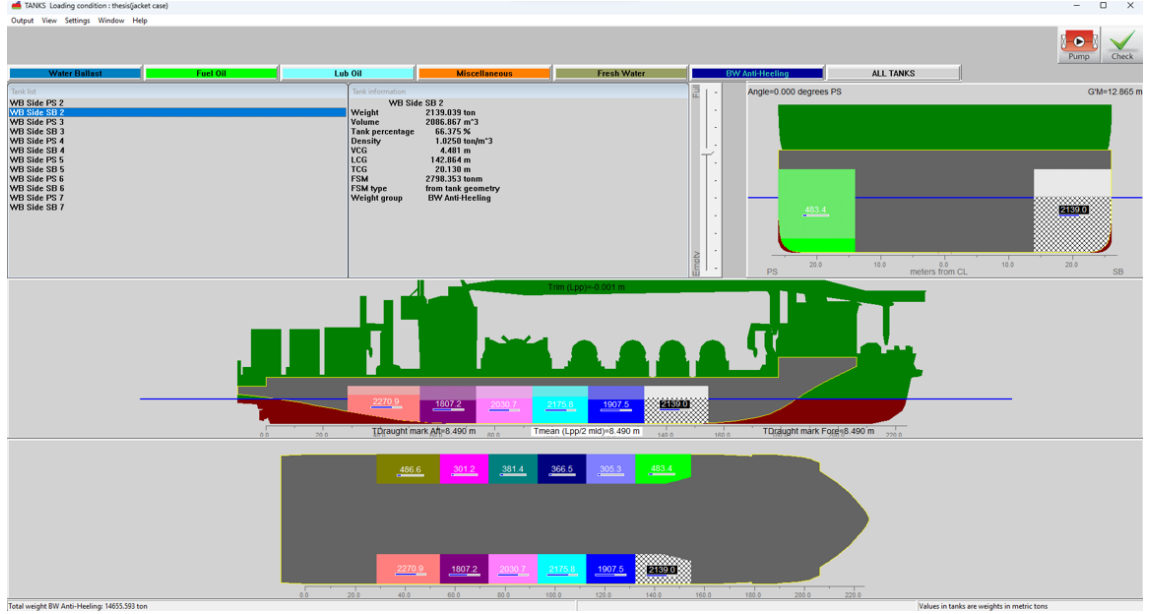
Figure 4.7: Sarc Pias general interface to interactively ballast the tanks

Interactive ballasting within the SARC software was conducted to achieve a balanced state where the vessel exhibited neither heel nor trim. Following these adjustments, the intact stability module of the SARC PIAS was engaged. This module evaluated the vessel's intact stability and provided output on the moment of inertia for all tanks and LCG, VCG, and TCG of vessel. These inertia calculations, alongside the previously determined inertias of other components, were then compiled into a spreadsheet. The moment of inertias with respect to vessel COG were calculated using steiner component/parallel axis theorem. Formulas are given in equation 4.5 to 4.7

$$I_{xx,G} = m[(VCG - VCG_{ship})^2 + (TCG - TCG_{ship})^2] + I_{xx,local} \tag{4.5}$$

$$I_{yy,G} = m[(VCG - VCG_{ship})^2 + (LCG - LCG_{ship})^2] + I_{yy,local} \tag{4.6}$$

$$I_{zz,G} = m[(LCG - LCG_{ship})^2 + (TCG - TCG_{ship})^2] + I_{zz,local} \tag{4.7}$$

The radius of gyration about x, y, and z axes are calculated using formulas given in equations 4.8 to 4.9

$$K_{xx} = \sqrt{\frac{I_{xx,G}}{m}} \tag{4.8}$$

$$K_{yy} = \sqrt{\frac{I_{yy,G}}{m}} \tag{4.9}$$

$$K_{zz} = \sqrt{\frac{I_{zz,G}}{m}} \tag{4.10}$$

After all these calculations, summary of hydrostatic paramteres was compiled and tabulated in table **??**. For further calculations, GM_{fluid} was calculated because of the fact that all the ballast tanks were not fully filled and due to this, there will be free surface moment effect which will reduce the metacentric height.

4.9 Sea Keeping Analysis

Seakeeping analysis is required to understand the motion responses of a vessel in reaction to waves. For this purpose, the hydrodynamic database of the vessel is determined using ANSYS-AQWA. AQWA is a 3D diffraction analysis suite used to investigate the effects of wave, wind, and current on floating and fixed offshore and marine structures. These structures include spars, FPSO systems, semi-submersibles, TLPs, ships, renewable energy systems, and breakwater designs. This software package is well recognized in the offshore and marine industry. Since the study involves lowering operations, no forward speed is included in the hydrodynamic database. Additionally, no heel and trim are included in the geometric model.

4.9.1 Hydrodynamic Model

The AQWA model of the vessel is created based on the 3D STEP model of Les Alizes. The mesh consists of approximately 4762 elements. An internal lid is specified to prevent irregular frequency problems. Figure 4.8 and 4.9 shows the AQWA model with the mesh elements.
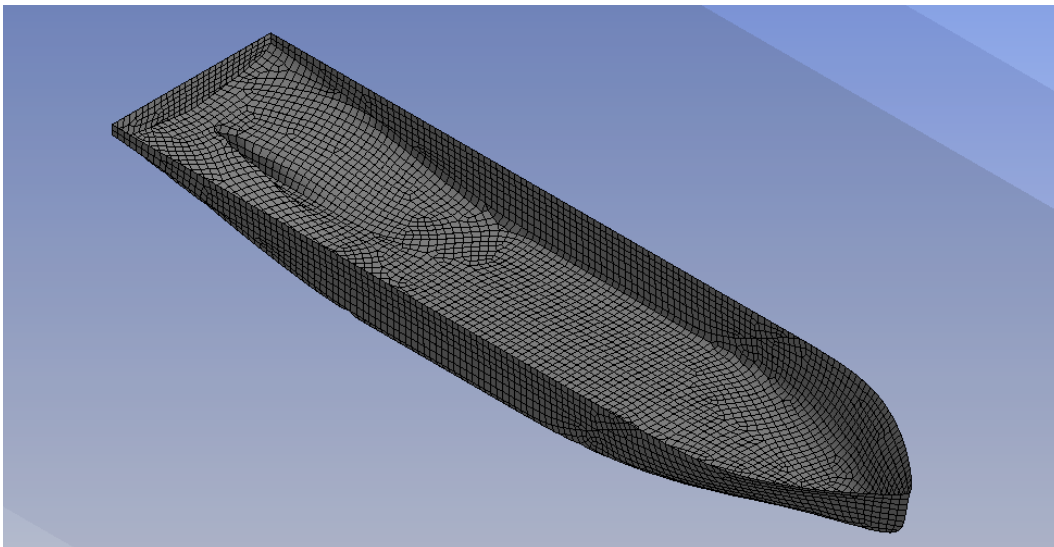
Figure 4.8: AQWA Mesh,isometric view
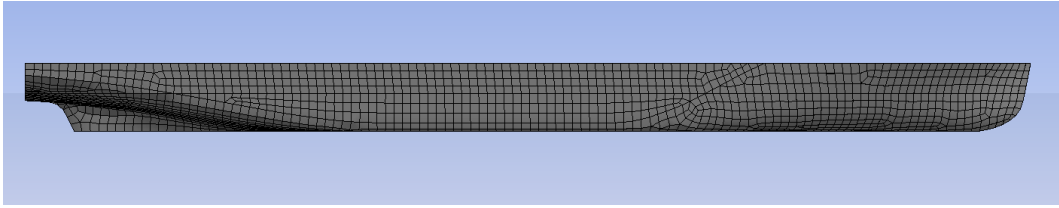
Figure 4.9: AQWA Mesh,profile view of the vessel.

4.9.2 Mesh Sensitivity Analysis

Mesh sensitivity analysis is usually performed in order to achieve convergence of the results so that an acceptable mesh size can be used for analysis. It indicates how changes in mesh size affect the result. A large mesh size can miss important details and results can be inaccurate. In contrast, very fine mesh size is able to capture excessive details at the expense of high computational time and processing power.

For this study, an acceptable mesh size is determined based on the tolerance limit of 0.1%. Maximum value of pitch RAOs at 0° is calculated for different mesh sizes starting from a coarse mesh of 3.5 m and reducing mesh size till a very fine mesh of 1 m. Results are evaluated and mesh size against which tolerance limit is achieved is used for further analysis. Details of this mesh independence study is mentioned in table 4.2. It can be seen that relative difference in pitch RAO results against mesh size of 2.5 m and 2 m reduces below 0.1%. So, mesh size having maximum cell length of 2 m is used for all further analysis. Roll RAOs are not used for mesh sensitivity analysis because potential solvers calculate undamped roll RAOs and values are unrealistic. So, pitch RAOs are calculated for wave angle of 0°.

Table 4.2: Mesh independence study details

Mesh Size(m)	Pitch RAO(degree/m)	% difference
3.5	0.7291	-
3	0.72993	0.114%
2.5	0.73069	0.104%
2	0.73116	0.064%
1.5	0.73135	0.026%
1	0.73144	0.012%

4.9.3 Hydrostatic Validation

The AQWA model mesh is validated for the given loading condition by comparing the hydrostatic data from the stability calculations (SARC) to the hydrostatic data of the AQWA model. The values are presented in the table below.

Table 4.3: Validation of the hydrostatic model in ANSYS AQWA

Parameter	Sarc	AQWA	Difference(%)
Displacement(t)	80003	80389	0.48
LCG(m)	106.42	106.80	0.35

4.9.4 Analyzed Wave Directions and Periods

Hydrodynamic analysis is performed for periods ranging from 3.5 seconds to 30 seconds in steps of 0.25 seconds. The wave directions considered range from -180° to 180° in steps of 15°.

4.9.5 Natural Period

Table **??** shows the natural periods of vessel for heave, roll, and pitch. These natural periods are calculated using the hydrodynamic diffraction model in ANSYS AQWA. Modal analysis of the model for the whole lifting arrangement is also done in Orcaflex. This analysis made clear that natural period of vessel and the whole lifting system does not coincide and there is no chance of resonance between them.

4.9.6 Potential and Viscous Damping

Hydrodynamic analysis in AQWA is conducted using 3D diffraction theory based on potential flow theory. This theory provides linear damping related to wave-making. For linear theory, horizontal modes of motion (surge, sway, and yaw) are typically out of resonance in common sea conditions, making damping less significant. Therefore, potential flow theory accurately evaluates the linear amplitudes of these motions.

Vertical modes of motion (heave, pitch, and roll) can enter linear resonance. The wave-making part of the damping is dominant for heave and pitch, resulting in good agreement

between experimental and numerical results from potential flow theory. However, for roll motion, nonlinear damping needs to be added to the analysis.

Whether to add additional roll damping depends on the likelihood of roll resonance occurring. This determination is based on comparing roll RAOs in beam seas with the natural sea state where the offshore operation will be performed. If the natural sea state coincides with the roll resonance period in beam sea conditions, additional roll damping is necessary and should be incorporated using the Ikeda method. If these conditions do not coincide, the analysis can proceed without adding viscous roll damping.

4.9.7 RAO Plots

The Roll RAO is computed for the center of gravity (COG) of the vessel, considering the cargo component list. This data is derived from the deck layout of the vessel, as detailed in appendix **??**, where the positions of all other components can also be verified.

The natural sea state at Borkum Riffgrund, where monopiles are to be installed, have waves with T_p ranging from 4 to 12 seconds. RAOs for each degree of freedom in various directions can be seen in appendix **??**. Figure 4.10 shows roll RAOs separately for beam sea condition and it can be seen that the resonance period for roll is approximately 22 seconds. As the natural sea state and the natural roll period do not align, there is no likelihood of resonance occurring. Therefore, there is no requirement for additional viscous damping in AQWA/ORCAWave.
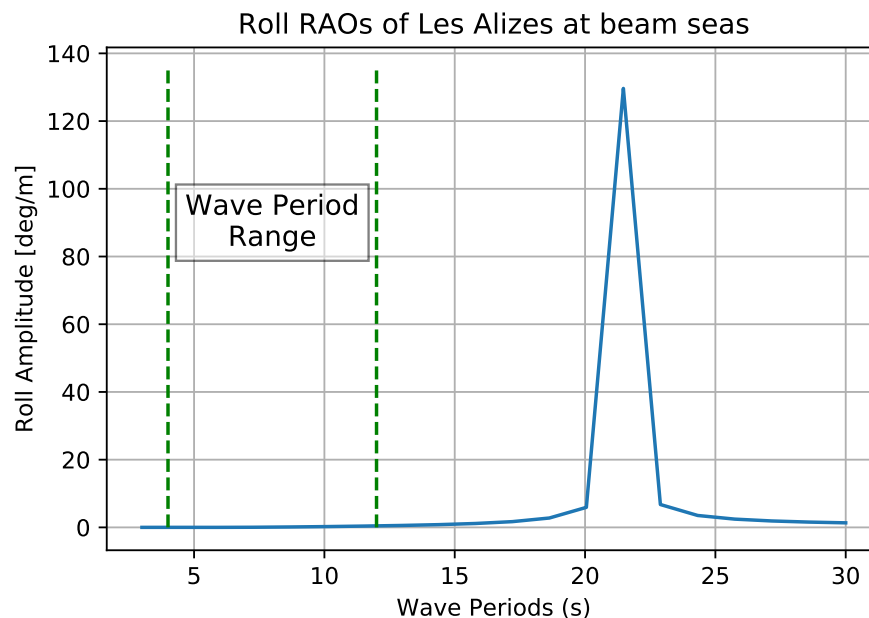

Figure 4.10: Vessel Roll RAOs at beam seas

4.10 Sea-state RAOs

Any object in the sea disturbs the sea conditions due to interactions with passing waves, such as wave radiation and diffraction. While small objects like buoys have minimal impact on
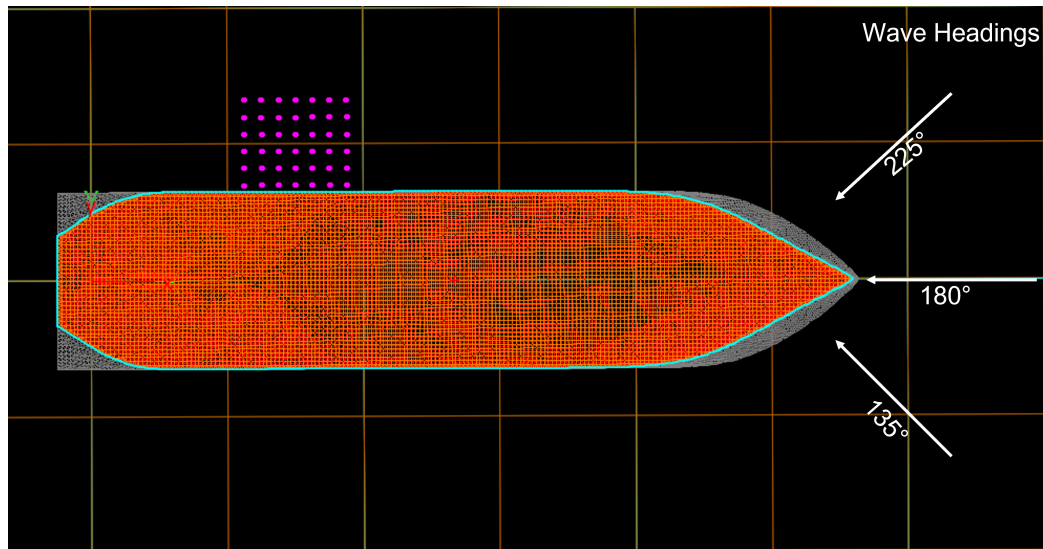
Figure 4.11: Sea State RAOs location

the sea state, large objects like vessels can significantly disturb nearby sea conditions.

We can model the disturbance effects of a vessel, referred to as the disturbance vessel, using sea state RAO data specific to the vessel type. These disturbance effects can be applied to nearby objects (monopile in this case). This feature is useful for modeling phenomenon like wave shielding, where objects behind a large vessel experience reduced wave action.

The sea state RAOs define the amplitude scaling and phase shift of the disturbed wave components relative to the incoming undisturbed waves, considering factors like position, wave direction, and period relative to the vessel. For dynamic analysis, Orcaflex requires velocity potential disturbance RAOs as input, as they provide more convenient manual data entry and ensure better interpolation performance [37].

We can obtain sea state RAO data from vessel motion diffraction analysis programs or input simple RAO data manually. For instance, we can model uniform scaling of wave amplitudes by entering a single RAO amplitude, which applies to all wave components and positions for objects linked to the disturbance vessel. Orcaflex utilizes interpolation to determine the appropriate sea state disturbance RAO for each wave component at any given position.

Sea state RAOs can be determined using either ANSYS AQWA Flow or Orcawave. For this work, sea state RAOs are computed for the splash zone where the monopile is intended to be positioned. These RAOs are derived for an area covering the entirety of the monopile's designated location, as indicated in the lifting plan provided earlier. The sea state disturbance is assessed at the waterline (z = 0) within the region defined by $45 \leq x \leq 75$ and $27 \leq y \leq 54$. Here, x, y, and z represent the positions relative to the vessel's origin, with x denoting the longitudinal position and y representing the transverse position. Specific points for evaluating sea state disturbance are depicted in Figure 4.11.

The presence of a vessel causes disturbances in the velocity potential of incoming waves due to diffraction and radiation effects. An analysis using a potential solver like ANSYS AQWA or Orcawave provides this disturbance potential, which is a combination of diffraction and

radiation effects. To distinguish between these effects, the analysis is conducted twice. First, the vessel is allowed to move freely, capturing the combined diffraction and radiation effects. Then, all degrees of freedom of the vessel are fixed, isolating the diffraction effect. The difference between these two analyses reveals the change in velocity potential attributed to radiation alone.

Figure **??** and **??** shows the change in velocity potential of incoming waves due to effect of radiation and diffraction separately. It can be seen that major contribution to alter the potential of incoming waves is due to diffraction and very minor contribution is due to radiation by the vessel. For any combinations of wave period and direction, we see an interference between diffracted and radiated waves and combined effect we see in the form of total disturbance experienced by the sea state in the splash zone location. But the major contribution in disturbing the sea state is due to diffraction.

Figure **??** illustrates the disturbance in velocity potential caused by the combined effect of diffraction and radiation resulting from the presence of the vessel. These sea state RAOs are computed for wave peak periods ranging from 4s to 12s and for heading angles between 135° and 225°. For incoming wave angles from 135° to 180°, there is a decrease in the amplitude of incoming waves, while for other heading angles, there is an increase in amplitude ratio. This phenomenon forms the basis of the shielding effect, demonstrating how the presence of the vessel alters the sea state and provides protection to the operational location against incoming waves.

4.11 Dynamic Analysis in Orcaflex

Orcaflex is the software package for the design and analysis of a wide range of marine systems. Typical applications in offshore dynamics include riser systems(SCRs, TTRs, hybrids, flexibles, umbilical, hoses), mooring systems(spread,turret,SPM,etty,etc.), marine renewables, installation planning with capabilities across the full range of scenarios, towed systems(bundle dynamics, seismic arrays, towed bodies, etc.), defence, seabed stability and many other types of systems. [38]

Time domain dynamic simulations have been performed in Orcaflex in order to simulate the complete behaviour of lowering oprations. These simulations require complete modeling of the system in Orcafle. Major modelling steps are discussed here.

4.11.1 Vessel Modelling in Orcafle

In Orcafle, a vessel is modeled using a set of data including the vessel's length, mass, COG location, moment of inertia tensor, displacement RAOs, load RAOs, sea state RAOs for the splash zone, stiffness, added mass, and damping matrices for all analyzed wave periods. Additionally, any other damping, such as viscous roll damping if required, as well as current loads, wind loads, and vessel drawings are included. This data is derived from previous diffraction analysis using a potential solver.

Subsequently, Orcafle needs to be informed about the types of loads the vessel will be evaluated against. In this study, the vessel was evaluated only against wave loads, added

mass, and damping. Wind loads are not included, as the goal is to compare shielded and unshielded sea states. Wind and current loads are second order slow drifting forces but this study is focused on first order loads (waves), so wind and current loads are neglected. Furthermore, neglecting wind loads in both cases ensures a consistent comparison, which is why they are omitted. Figure 4.12 shows the Orcaflex menu where this data is to be entered.
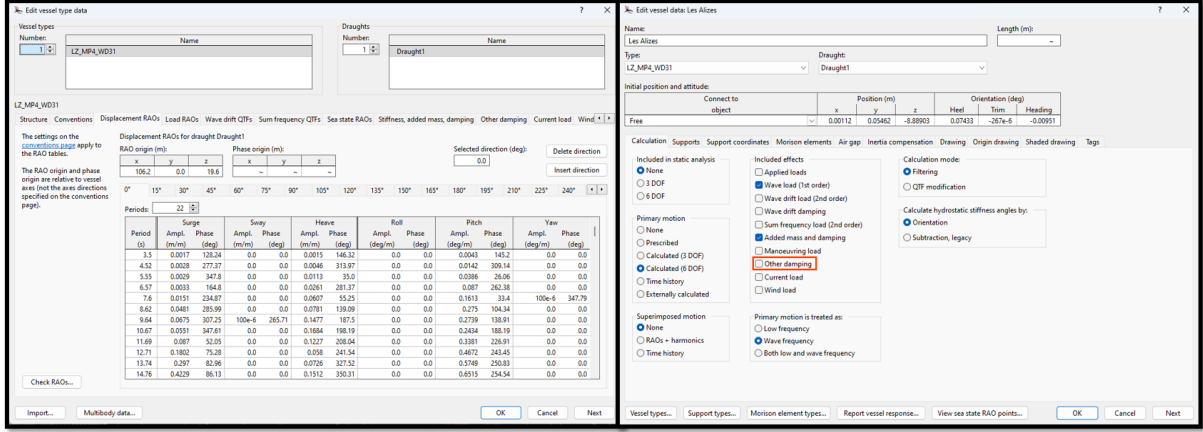
Figure 4.12: Vessel Data Form in Orcaflex

4.11.2 Monopile Modelling in Orcaflex

Monopile modeling in Orcaflex is carried out by inputting the accurate geometry of the monopile, including the correct section length and diameter. The monopile is represented as a spar buoy (circular cross-section) with multiple sections in Orcaflex. For this, the outside diameter of each section, inside diameter of each section, and length of each section are input into Orcaflex. Additionally, the added mass and drag coefficients are included, based on DNV RP C205 [39].

The moment of inertia for each section of the monopile is calculated individually and then adjusted to the global centroid of the monopile using the following formulas.

The local moment of inertia for each cylinder, given its length (l), breadth (b), and height (h), is calculated using the formulas in equations 4.11 to 4.13.

$$I_{xx,local} = \frac{1}{12}(b^2 + h^2)m \tag{4.11}$$

$$I_{yy,local} = \frac{1}{12}(l^2 + h^2)m \tag{4.12}$$

$$I_{zz,local} = \frac{1}{12}(l^2 + b^2)m \tag{4.13}$$

The moments of inertia with respect to the monopile's center of gravity (COG) are calculated using the parallel axis theorem, as shown in equations 4.14 to 4.7.

$$I_{xx,COG} = m[(VCG - VCG_{mp})^2 + (TCG - TCG_{mp})^2] + I_{xx,local} \tag{4.14}$$

$$I_{yy,COG} = m[(VCG - VCG_{mp})^2 + (LCG - LCG_{mp})^2] + I_{yy,local} \tag{4.15}$$

$$I_{zz,COG} = m[(LCG - LCG_{mp})^2 + (TCG - TCG_{mp})^2] + I_{zz,local} \tag{4.16}$$

Next, the connection of the monopile in Orcaflex is specified as free, and the disturbance vessel for the monopile, which in this case is Les Alizes, is selected. This ensures that Orcaflex accurately models and transmits the disturbances created by the vessel's presence in the sea state to the monopile being lowered into the splash zone. Figure **??** shows the monopile drawing.

4.11.3 Jacket Modelling in Orcaflex

Jacket modeling in Orcaflex is carried out by inputting the accurate geometry of the jacket. The members of the jacket are represented by line objects in Orcaflex. For these line objects, outside and inside diameter, youngs modulus, bending stiffness, axial stiffness, poisson ratio, torsional stiffness, normal and axial drag coefficients, and added mass coefficients are specified in Orcaflex. The mass of the whole jacket and mass moments of inertias are respresented by a reference buoy and every line object is connecte to this reference buoy in Orcaflex. The mass and moment of inertias of jacket are tabulated in **??**

4.11.4 Environment Modelling

After completing the equipment modeling and inputting the required values for dynamic analysis in Orcaflex, the next step involves environmental modeling to accurately replicate the realistic sea state where the operation is performed. This process includes inputting various wave parameters such as wave spectrum, wave direction, wave height, and wave peak period.

To accurately reflect the actual sea state and its impact on the lowering operation, it is necessary to incorporate waves with all possible peak periods, wave headings, and wave heights that are likely to occur. This way of applying the probable sea state will make sure that analysis incorporates all the possible scenarios which can occur during the operation.

To take this into account, various parameters that suggest the type of environment are used in the simulations to make sure that realistic operational analysis is performed. JONSWAP spectrum is used and it is realistic for this study because Borkum Riffgrund 3 is located in german north sea and JONSWAP spectrum is also valid for north sea.

Following environmental parameters are used to asses the lowering in Orcaflex

Table 4.4: Wave Parameters Summary

Parameter	Value
Directions	135° to 225°
Maximum Wave Height	2.5m
Wave Spectrum	JONSWAP
Peak Periods	4s to 12s
Peak enhancement factor γ	Variable
Water Depth	33.5m
Sea Bed	Flat

While modeling the wave spectrum itself, Orcaflex uses the formula from isherwood [40] in order to evaluate the peak enhancement factor γ. But in this thesis, γ is evaluated by using the formulas stated in the recommended practice by DNV RP C205 [39]. Based on this recommended practice, value of γ is dependent on the ratio of wave peak period T_p to the square root of significant wave height H_s. Formulas in equation 4.17 to 4.19 state the guidelines for γ value.

$$\gamma = 5 \quad \text{for} \quad \frac{T_p}{\sqrt{H_s}} \leq 3.6 \tag{4.17}$$

$$\gamma = exp(5.75 - \frac{1.15 \cdot T_p}{\sqrt{H_s}}) \quad \text{for} \quad 3.6 \leq \frac{T_p}{\sqrt{H_s}} \leq 5 \tag{4.18}$$

$$\gamma = 1 \quad \text{for} \quad \frac{T_p}{\sqrt{H_s}} \geq 5 \tag{4.19}$$

Dynamic simulations in Orcaflex are run at a maximum wave height of 2.5 m. Other than 2.5 m, simulations are run at 1.5 m as well. By using results at these two wave heights, if needed, results can be evaluated at any other intermediate wave height using interpolation. The type and relevant formulas for interpolation are discussed in results processing.

For these two wave heights, seven different wave directions and nine different wave peak periods are utilized for dynamic simulations. Moreover, having all these environmental conditions combinations, three different monopile drafts are used for which simulations are run. And for each draft, all the simulations are run for both shielded and unshielded splash zone. Summing up all these combinations, a total of 750 simulations are performed.

To run these 750 simulations one by one, the data file of Orcaflex needs to be updated everytime before running the simulation. Because of the fact that γ also changes for different values of $\frac{T_p}{\sqrt{H_s}}$, it also needs to be varied everytime. Doing these changes before running every simulation is a cumbersome task and involves a lot of manual labour.

To speed up this process and lessen the manual data entry, a python script is employed to get this job done. The script on its own updates the data file by changing the environmental parameters and γ values according to equations 4.17 to 4.19 and saves individual data files for every case. In this way the file generation process becomes faster and much time can be saved.

Although generating all the simulation cases using python script makes the task easier but still opening Orcaflex and running each file and then closing it and running again the next file needs constant attention and it will take a lot of time to finish all these simulations. To overcome this batch processing feature in Orcaflex is used in which all the simulation files can be loaded all at once and Orcaflex uses all the processing cores to solve the dynamics for 12 cases simultaneously and then next 12 until all finish. This doesn't require constant human attention.

Figures 4.13 and 4.14 shows the Orcaflex model with all the equipments in case case of monopile and jacket installation.
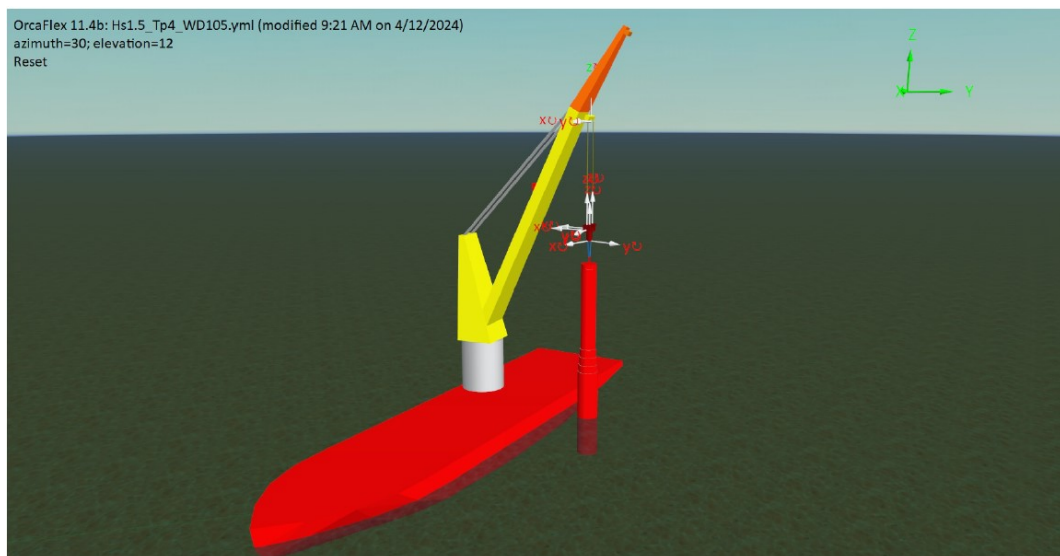

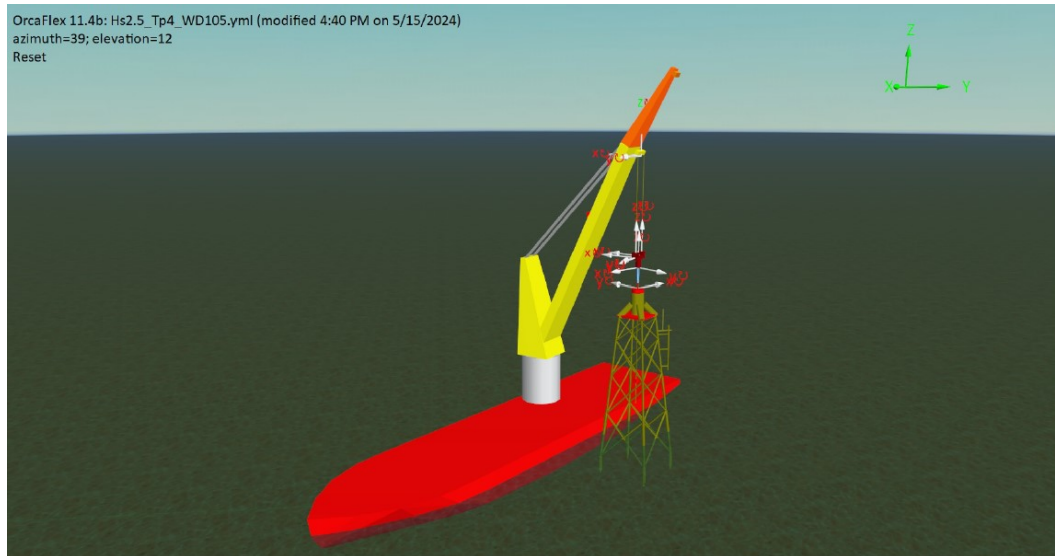**Figure 4.13:** Orcaflex monopile installation shaded graphics model

Figure 4.14: Orcaflex jacket installation shaded graphics model

4.12 Results Processing

Orcaflex spreadsheet is employed in order to extract results of monopile motion, crane DAF, and crane leads. These results are retrieved against wave T_p and directions specified in table 4.4. This spreadsheet works by first taking any simulation file as an input and then user can specify which results are needed and then these required results can be duplicated for each case. Parallel processing can also be used in Orcaflex spreadsheet so as to speed up the process of results extraction to save time.

Once all the results are done, they can be compiled according to different classes. For example, based on monopile draft, based on significant wave height, based on splash zone i.e. shielded or not shielded. The data is compiled in this manner in order to have proper reference to use it afterwards.

The simulations are conducted for wave heights of 1.5 m and 2.5 m. After obtaining the results, each value is compared against its corresponding limit value as specified in table 4.1. If the results exceeded the permissible limits, the significant wave height is adjusted downwards to comply with the limiting criteria. This adjustment is achieved through quadratic interpolation, using results from the static state (0 m wave height), 1.5m wave height, and 2.5m wave height as input data.

Rather than rerunning the simulations for a lower wave height each time to check if the results meet the corresponding limits, the interpolation method is used to determine the necessary reduction in wave height to ensure all results are within their limits. Specifically, simulations are conducted for wave heights of 1.5m and 2.5m, and we also have the static state results corresponding to a wave height of 0m. This provides us with three data points to work with. For instance, when evaluating the crane DAF results, the three data points would be: $(0, \text{daf}_0)$, $(1.5, \text{daf}_{1.5})$, and $(2.5, \text{daf}_{2.5})$. If DAF becomes more than its limiting criteria of 1.15, because we have three points to interpolate, quadratic interpolation can be utilized in order to correctly approximate the value of allowable wave height for which DAF

doesn't exceed 1.15.

So to have quadratic interpolation, a quadratic equation is needed which should satify the three points stated above. This equation can have the form y = ax^2 + bx + c. To derive this equation value of coefficients a, b, and c are needed. These coefficients can be determined using the following formulas derived from the given points as shown in equations 4.20 to 4.22

$$a \; = \; \frac{x_1 \cdot (y_3 - y_2) \; + \; x_2 \cdot (y_1 - y_3) \; + \; x_3 \cdot (y_2 - y_1)}{(x_1 - x_2)(x_1 - x_3)(x_2 - x_3)} \tag{4.20}$$

$$b \; = \; \frac{y_2 - y_1}{x_2 - x_1} \; - \; a \cdot (x_1 + x_2) \tag{4.21}$$

$$c \; = \; y_1 - ax_1^2 - bx_1 \tag{4.22}$$

Benefit of using this interpolation method is that it will approximate the results better than linear interpolation and also because no need to run simulations for intermediate values of H$_s$. This will save considerable amount of time as extra simulations need not to be run.

At this step, the significant wave height is already calculated against each of the limiting criteria separately. But we know that during operation, all of the stated limiting criteria will effect the lifting operation. So, it is needed that significant wave height should be calculated which should incorporate all the three limiting criteria simultaneously. For this purpose, it is required to find out the governing criterion among all the limiting criteria.

To find the governing limiting criterion, we need to study results for each case separately and check the result against which significant allowable wave height is least. This particular result is governing the wave height for that specific period and wave direction. This dictates how high should be wave in order to limit the operation within limits. If these steps are taken into account and taken care of while planning the operation, the whole installation operation is well within its safe limits.

After compiling all the results for each scenario, workability pivot tables are created for both shielded and unshielded splash zones. The effectiveness of employing shielding during operation planning is evaluated by calculating the ratio of allowable wave heights for shielded versus unshielded splash zones. This analysis is repeated for all three monopile drafts to ensure comprehensive coverage.

At this step, workability plots can be created for every case. Workability plots are created based on the classification of results as discussed above. Most important is to make these pivot plots for shielded splash zone and unshielded splash zone. Then in order to make a compatible comparison, the ratio of significant wave height is taken in case of shielded to unshielded splash zone. Similarly these pivot tables of workability are made for each draft separately. The advantage of data representation using pivot table is the clear understanding of the results for every individual wave height and wave peak period combination. It also simplifies the comparison.

By comparing the ratios of allowable wave heights, we can tell pin point that at which sea

state, sheilding is assisting the operation. The pivot tables and heat maps provide a detailed yet accessible way to interpret the data, ensuring that all aspects of the analysis are easily understood.

5
Conclusion and Future Scope

In this section, the main points and findings of the study are put togeher. This provides a clear summary of the steps that are taken and what is learned becuase of this study. By gathering all this information in one place, the overall significance of this work can be appreciated. In the end, future scope is written as to what more can be done in this regard.

Conclusions

- The challenges in offshore lifting operations, such as the exposure of lifting systems to wave-generated forces during foundation installation and the risk of pendulum-like movements during turbine installations, necessitate the importance of detailed response analysis and proper operational planning. Any methods to improve the workability also improves the safety of the operation.

- This thesis investigated the effect of vessel shielding thoroughly to enhance the workability of offshore lifting operations. The findings show that positioning the vessel in such a way so as to block the impact of incoming waves produce quite calmer sea state which is quite feasible for offhosre lifting and installation operations.

- It can be concluded that shielding effect reduces the effect of incoming waves by reducing the monopile response in shorter waves. But in shorter waves, vessel itself does not move so much.

- If shielding effect is considered, the best heading angle that increases the workability limit ranges from bow quartering waves incoming from starboard side to nearly head seas(specific according to lifting plan considered in this thesis).

- Vessel shielding is more effective for diagonal waves because of the fact that diagonal waves encounter longer length of the vessel as compared to beam waves. So, for higher peak periods, shielding effect will be more effective for waves incoming from diagonal direction.

- Shielding decreases the workability limit(H_s) for waves ranging from head seas to bow quartering portside. So it has positive as well as negative effect depending on heading condition.

- The effect of vessel shielding is also dependent on monopile submergence height. More the submergence, less will be the workability enhancement for wave angles 135° to 165° and more will be the workability enhancement for wave angles of 195° to 225°. So, depending on what draft at which monopile is to be lowered, vessel position can be adjusted to have the highest allowable significant wave height.

- The workability is most sensitive to changes in crane offlead and sideleads. So these paramteres are governing the allowable wave height in this study.

- Shielding happens due to change in velocity potential of the incoming waves due to presence of vessel. Sea state changes because waves get diffracted due to vessel in their way and radiated because of the vessel motion.

- The predominant factor affecting changes in sea state is diffraction, because of the presence of the vessel, with a more pronounced effect observed for shorter wave periods. On the other hand, radiation effects are considerably less significant in altering sea state conditions. These effects primarily manifest during longer wave periods when the vessel's motion is more.

- As compared to monopiles, shielding effect is quite insignificant for jacket installation except for very few wave periods and directions because of the unequal distribution of sea state disturbance around the jacket geometry. So shielding can be ignored for jacket installation.

Future Work

- The approach followed in this thesis is based on Morison's formula in which monopile is treated as hydrodynamically transparent structure. But for bigger sizes, it would not behave as a morison element. For that, MP is to be treated as a diffracting body. Separate RAOs for monopile also needs to be calculated and multi-body analysis needs to be done in Orcaflex. So, in future, multi-body analysis in which vessel and MP both interact with each other can be analyzed to extend this study for larger structure sizes.

- In this study, only waves loads are studied. Wind and current loads are ignored. These loads can alter the average inclination of MP during operation. This can be modelled and analyzed to make the lowering operation more realistic in future.

- Furthermore, this study only incorporates one loading condition of the vessel (one vessel draft only). Multiple drafts of vessel can be studied in future to have the effect of vessel draft on shielding performance. In this way, optimal draft of the vessel can be ascertained which will react best to the shielding performance of the vessel.

- This analysis is based only on the foundation installation. It can be extended to turbine rotor and nacelle installation as well. Installation analysis of all these components including foundation and RNA can help in planning the installation of complete windfarm.

Bibliography

[1] WindEurope. windeurope.org. `https://windeurope.org/wp-content/uploads/files/about-wind/statistics/WindEurope-Annual-Offshore-Statistics-2019.pdf`, 2019. [Accessed 27-05-2024].

[2] Christopher Moné, A Smith, Ben Maples, and M Hand. 2013 cost of wind energy. *National Renewable Energy Laboratory: Golden CO*, 2015.

[3] IEA. Technology Roadmap - Wind Energy 2013 – Analysis - IEA — iea.org. `https://www.iea.org/reports/technology-roadmap-wind-energy-2013`, 2013. [Accessed 27-05-2024].

[4] Zhiyu Jiang. Installation of offshore wind turbines: A technical review. *Renewable and Sustainable Energy Reviews*, 139:110576, 2021.

[5] EWEA. ewea.org. `https://www.ewea.org/fileadmin/files/library/publications/statistics/EWEA-European-Offshore-Statistics-2015.pdf`, 2015. [Accessed 27-05-2024].

[6] Tony Burton, Nick Jenkins, David Sharpe, and Ervin Bossanyi. *Wind energy handbook*. John Wiley & Sons, 2001.

[7] Erich Hau and Erich Hau. The wind resource. *Wind Turbines: Fundamentals, Technologies, Application, Economics*, pages 505–547, 2013.

[8] J. Twidell and G. Gaudiosi. *Offshore Wind Power*. Multi-Science Publishing Company, 2009. ISBN 9780906522639. URL `https://books.google.be/books?id=zfcLPQAACAAJ`.

[9] Eu offshore wind. Offshore Wind in Europe Key Trends and Statistics 2020 | The European Maritime Spatial Planning Platform — maritime-spatial-planning.ec.europa.eu. `https://maritime-spatial-planning.ec.europa.eu/practices/offshore-wind-europe-key-trends-and-statistics-2020#:~:text=Europe%20now%20has%20a%20total,start%20in%20the%20coming%20years.`, 2020. [Accessed 27-05-2024].

[10] Chia Chen Ciang, Jung-Ryul Lee, and Hyung-Joon Bang. Structural health monitoring for a wind turbine system: a review of damage detection methods. *Measurement science and technology*, 19(12):122001, 2008.

[11] GAM Van Kuik, Joachim Peinke, Rogier Nijssen, Denja Lekou, Jakob Mann, Jens Nørkær Sørensen, Carlos Ferreira, Jan-Willem van Wingerden, David Schlipf, Pieter Gebraad, et al. Long-term research challenges in wind energy–a research agenda by the european academy of wind energy. *Wind energy science*, 1(1):1–39, 2016.

[12] Kurt Thomsen. *Offshore wind: a comprehensive guide to successful offshore wind farm installation*. Academic Press, 2014.

[13] Kenneth Peire, Hendrik Nonneman, and Eric Bosschem. Gravity base foundations for the thornton bank offshore wind farm. *Terra et Aqua*, 115(115):19–29, 2009.

[14] Walter Musial, Sandy Butterfield, and Bonnie Ram. Energy from offshore wind. In *Offshore technology conference*, pages OTC–18355. OTC, 2015.

[15] annevisser. Seaway Installs Sylwin Alpha Converter Platform — offshorewind.biz. `https://www.offshorewind.biz/2014/07/14/seaway-installs-sylwin-alpha-converter-platform/`, 2014. [Accessed 28-05-2024].

[16] SA Herman. Offshore wind farms. analysis of transport and installation costs. 2002.

[17] Alternative foundation installation techniques. flow-offshore.nl. `https://flow-offshore.nl/images/flow-openbaar/alternative-foundation-installation.pdf`, 2011. [Accessed 28-05-2024].

[18] Sarkar. Installation of monopiles for offshore wind turbines—by using end-caps and a subsea holding structure. In *International Conference on Offshore Mechanics and Arctic Engineering*, volume 44373, pages 309–315, 2011.

[19] Kenneth Aarset, Arunjyoti Sarkar, and Daniel N Karunakaran. Lessons learnt from lifting operations and towing of heavy structures in north sea. In *Offshore Technology Conference*, pages OTC–21680. OTC, 2011.

[20] Robert B Gordon, Guttorm Grytøyr, and Mayuresh Dhaigude. Modeling suction pile lowering through the splash zone. In *International Conference on Offshore Mechanics and Arctic Engineering*, volume 55317, page V001T01A010. American Society of Mechanical Engineers, 2013.

[21] Mateusz Graczyk and Peter Christian Sandvik. Study of landing and lift-off operation for wind turbine components on a ship deck. In *International Conference on Offshore Mechanics and Arctic Engineering*, volume 44946, pages 677–686. Citeseer, 2012.

[22] MJ Perry and PC Sandvik. Identification of hydrodynamic coefficients for foundation piles. In *ISOPE International Ocean and Polar Engineering Conference*, pages ISOPE–I. ISOPE, 2005.

[23] Remmelt Van der Wal, Hans Cozijn, and Chris Dunlop. Model tests and computer simulations for njord fpu gas module installation. In *Proceedings of the Marine Operations Speciality Symposium (MOSS)*, 2008.

[24] Peter Chr Sandvik. Estimation of extreme response from operations involving transients. In *Second Marine Operations Specialty Symposium (MOSS), Singapore, Aug*, pages 6–8, 2012.

[25] PK Mukerji. Hydrodynamic responses of derrick vessels in waves during heavy lift operation. In *Offshore Technology Conference*, pages OTC–5821. OTC, 1988.

[26] HJJ Van den Boom, JN Dekker, and RP Dallinga. Computer analysis of heavy lift operations. In *Offshore Technology Conference*, pages OTC–5819. OTC, 1988.

[27] JJM Baar, JGL Pijfers, and JA van Santen. Hydromechanically coupled motions of a crane vessel and a transport barge. In *Offshore Technology Conference*, pages OTC–6949. OTC, 1992.

[28] Zhen, Lin Moan, Li, Torgeir Gao, and Harald Ormberg. Analysis of lifting operation of a monopile for an offshore wind turbine considering vessel shielding effects. *Marine structures*, 39:287–314, 2014.

[29] DNV DNV-RP. C205 environmental conditions and environmental loads. *Det Norske Veritas: Oslo, Norway*, 2010.

[30] W Bai, MA Hannan, and KK Ang. Numerical simulation of fully nonlinear wave interaction with submerged structures: Fixed or subjected to constrained motion. *Journal of Fluids and Structures*, 49:534–553, 2014.

[31] Harald. Analysis of lifting operation of a monopile for an offshore wind turbine considering vessel shielding effects. *Marine structures*, 39:287–314, 2014.

[32] Lin Li, Zhen Gao, and Torgeir Moan. Response analysis of a nonstationary lowering operation for an offshore wind turbine monopile substructure. *Journal of offshore mechanics and Arctic engineering*, 137(5):051902, 2015.

[33] Det Norske Veritas. Modelling and analysis of marine operations. *Offshore Standard*, 80, 2011.

[34] Lin Li, Zhen Gao, and Torgeir Moan. Comparative study of lifting operations of offshore wind turbine monopile and jacket substructures considering vessel shielding effects. In *ISOPE International Ocean and Polar Engineering Conference*, pages ISOPE–I. ISOPE, 2015.

[35] Torgeir. Comparative study of lifting operations of offshore wind turbine monopile and jacket substructures considering vessel shielding effects. In *ISOPE International Ocean and Polar Engineering Conference*, pages ISOPE–I. ISOPE, 2015.

[36] JDN. jandenul.com. `https://www.jandenul.com/sites/default/files/2020-06/Les%20Aliz%C3%A9s%20%28EN%29_.pdf`, 2020. [Accessed 29-05-2024].

[37] Orcina. Vessel types: Sea state disturbance RAOs — orcina.com. `https://www.orcina.com/webhelp/OrcaFlex/Content/html/Vesseltypes,SeastatedisturbanceRAOs.htm`. [Accessed 03-06-2024].

[38] ORCINA. OrcaFlex - dynamic analysis software for offshore marine systems — orcina.com. `https://www.orcina.com/orcaflex/`. [Accessed 14-07-2024].

[39] DNV. Recommended practice dnv-rp-c205: environmental conditions and environmental loads. *DNV, Norway*, 2010.

[40] RM Isherwood. A revised parameterisation of the jonswap spectrum. *Applied ocean research*, 9(1):47–50, 1987.

[41] ewea. ewea.org. `http://www.ewea.org/fileadmin/files/library/publications/statistics/European_offshore_statistics_2013.pdf`, 2013. [Accessed 27-05-2024].

[42] Ryan Wiser, Zhenbin Yang, Maureen Hand, Olav Hohmeyer, David Infield, Peter H Jensen, Vladimir Nikolaev, Mark O'Malley, Graham Sinden, Arthouros Zervos, et al. Wind energy. *Renewable Energy Sources and Climate Change Mitigation*, pages 535–608, 2011.